BIOCHEMISTRY
including biophysical chemistry & molecular biology
Article

Biochemistry **2010,** *49,* 9199–9206 9199
DOI: 10.1021/bi101062v

Azole Drugs Trap Cytochrome P450 EryK in Alternative Conformational States[†,‡]

Linda Celeste Montemiglio, Stefano Gianni, Beatrice Vallone, and Carmelinda Savino*

Department of Biochemical Sciences, "Sapienza" University of Rome and CNR Institute of Molecular Biology and Pathology, P. le A. Moro 5, 00185 Rome, Italy

Received July 2, 2010; Revised Manuscript Received September 15, 2010

ABSTRACT: EryK is a bacterial cytochrome P450 that catalyzes the last hydroxylation occurring during the biosynthetic pathway of erythromycin A in *Streptomyces erythraeus*. We report the crystal structures of EryK in complex with two widely used azole inhibitors: ketoconazole and clotrimazole. Both of these ligands use their imidazole moiety to coordinate the heme iron of P450s. Nevertheless, because of the different chemical and structural properties of their N1-substituent group, ketoconazole and clotrimazole trap EryK, respectively, in a closed and in an open conformation that resemble the two structures previously described for the ligand-free EryK. Indeed, ligands induce a distortion of the internal helix I that affects the accessibility of the binding pocket by regulating the kink of the external helix G via a network of interactions that involves helix F. The data presented thus constitute an example of how a cytochrome P450 may be selectively trapped in different conformational states by inhibitors.

Cytochromes P450 (P450s)[1] represent a class of heme-containing monoxygenases that catalyze the oxidative metabolism of a wide number of endogenous and exogenous organic compounds (*1*−*4*). Their universal phylogenetic distribution and their involvement in many primary and secondary metabolic pathways allowed to exploit them as alternative targets for drug development in antimicrobial therapy as well as in treatment of metabolic disorders and cancer (*5*−*7*). Despite the common fold, it is to date difficult to predict P450−ligand interactions as well as the conformational change that binding may imply (*7*). In this context, structural analysis provides a tool to detect determinants for inhibitor binding (*8*).

Azole compounds are potent inhibitors of P450s. Among them, ketoconazole (KC) and clotrimazole (CLT) (Figure 1) are two synthetic azole drugs widely used for treatment of fungal and yeast infections (*9*).

The binding mechanism by which azole compounds can inhibit P450s has been extensively studied. In the case of imidazole derivative compounds, such as KC and CLT, the N3 of the imidazole ring binds directly to the heme iron as a sixth ligand, replacing a water molecule. This interaction stabilizes the low-spin iron configuration and prevents the binding of the substrate, causing the heme center to be inactive (*10*). However, even in the presence of such underlying common mechanism, specificity, affinity, and inhibition depend on the substituent group on the N1 of the azole molecule and on the interactions that it establishes with the amino acids in the active site of each specific P450 (*5*, *10*−*14*).

The C12-hydroxylase EryK is the last P450 acting during erythromycin A biosynthesis, performed by the actinomycete *Streptomyces erythraeus* (*15*). Structural and biophysical studies showed that, in order to perform the highly regio- and stereospecific hydroxylation of its large substrate, erythromycin D (ErD) (Figure 1), EryK evolved novel structural features with respect to related P450s (*16*). Following a conformational selection-like mechanism, the open conformer of EryK recognizes its substrate, ErD, closes, and locks around it. The crucial element of this mechanism is represented by a network of interactions (called HSWP network from the four amino acids involved: His243, Ser166, Trp165, Pro192) that connects helices I, F, and G, the latter being responsible for opening and closure of the active site. The geometry assumed by the residues belonging to the HSWP network regulates locking of EryK by altering the kinking of helix G. This network is also responsible for the stabilization of the open form of ligand-free EryK by keeping helix G straight. On the other hand, when the specific substrate ErD binds to the enzyme, helix I bends upon the pressure of the macrolactone ring. This conformational change causes the HSWP network to rearrange, stabilizing a kink of helix G that closes the active site, preventing its reopening until the release of the catalytic product. The HSWP network was not found to be set up in the closed form of ligand-free EryK (*16*).

In this work we studied two azole inhibitors of P450s in order to investigate the effect of the N1-substituent group on binding to a specific bacterial P450. We found KC and CLT to bind EryK with an affinity higher than that of ErD. The analysis of the crystal structures of the complexes with these inhibitors showed

[†]We are grateful to synchrotrons ESRF (beamline ID14.3, Grenoble, France) and BESSY (beamline ID14.1, Berlin, Germany). The European Community—Research Infrastructure Action under the FP7/2007-2013 under grant agreement no. 226716 is acknowledged. The work was supported by grants from Italian MIUR FIRB2003 RBLA03B3KC_004 and CNR RSTL2007-856.

[‡]The atomic coordinates and the structure factors were deposited under the codes 2JJP (structure of a cytochrome P450 EryK in complex with inhibitor ketoconazole (KC)) and 2XFH (structure of cytochrome P450 EryK cocrystallized with inhibitor clotrimazole) in the Protein Data Bank Research Collaboratory for Structural Bioinformatics, Rutgers University, New Brunswick, NJ (http://www.rcsb.org).

*To whom correspondence should be addressed. E-mail: linda.savino@uniroma1.it. Telephone: 39 06 49910548. Fax: 39 06 4440062.

[1]Abbreviations: EryK, erythromycin D C12-hydroxylase; P450, cytochrome P450; KC, ketoconazole; CLT, clotrimazole; ErD, erythromycin D; DMSO, dimethyl sulfoxide; KC-EryK, EryK in complex with KC; CLT-EryK, EryK in complex with CLT; K_d, dissociation constant; ErD-EryK, EryK in complex with ErD; rmsd, root-mean-square deviation.

Published on Web 09/16/2010

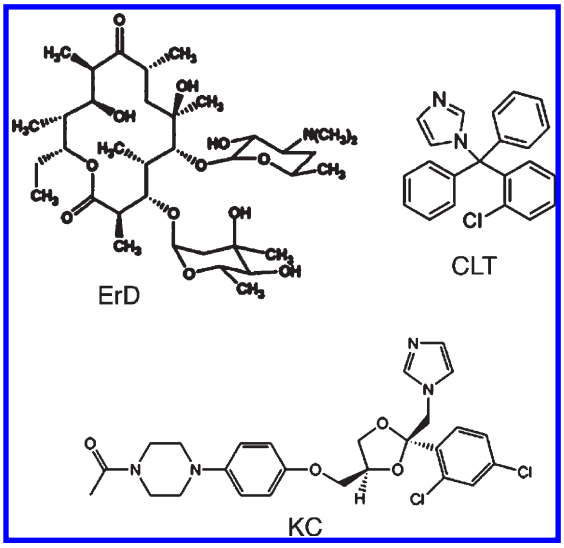

FIGURE 1: Chemical structures of the substrate of EryK, erythromycin D (ErD), and of the two azole antifungal compounds clotrimazole (CLT) and ketoconazole (KC).

that KC and CLT arrange differently into the active site of EryK, depending on their shape and flexibility. In both cases, the presence on the heme of the imidazole group directly bound to the iron induces a pronounced distortion of the long and flexible helix I. Depending on the bulk of the ligand, this structural modification affects the HSWP network, leading EryK to assume two conformations that resemble respectively its closed and open ligand-free structures.

This finding suggests that the presence of different conformational states is an additional factor to be considered in the analysis of substrate affinity and in the design of inhibitors. Such behavior has been recently observed on other P450s (*12*, *17*−*20*). Thus, EryK represents an example of a P450 that may be selectively trapped in a specific conformational state with optimized inhibitors.

The details on the structural arrangement of the active site of EryK and its importance as a model to gain new insight into molecular determinants of ligand binding to P450s as a conformational selection process will be also discussed.

EXPERIMENTAL PROCEDURES

Protein Expression and Purification. Recombinant His-tagged EryK wild type was overexpressed in BL21 STAR (DE3) *Escherichia coli* strain (Invitrogen, Carlsbad, CA) and purified as previously reported (*21*).

Sample Preparation and X-ray Data Collection. KC and CLT (Sigma Aldrich, St. Louis, MO) stock solutions (respectively 0.2 and 0.01 M) were prepared by dissolving them respectively in ethyl alcohol and dimethyl sulfoxide (DMSO). Crystals of EryK in complex with KC and CLT were obtained by cocrystallizing the protein (316 μM, 15 mg/mL) with 0.9 mM KC and 0.9 mM CLT, using the hanging-drop vapor diffusion method at 294 K (for more details see Table 1).

The diffraction data of EryK in complex with KC (KC-EryK) and with CLT (CLT-EryK) were collected at 100 K respectively at ESRF (Grenoble, France) beamline ID14.3 and at BESSY (Berlin, Germany) beamline ID14.1, using a *mar*CCD detector. KC-EryK data were integrated and scaled using the HKL suite (*22*); CLT-EryK data were processed using the HKL2000 suite (*23*).

Structure Determination and Refinement. The crystals of KC-EryK were isomorphous with the reported ligand-free closed crystals of EryK (PDB accession code 2JJN (*16*, *21*)); therefore, the atomic coordinates of the ligand-free closed form were used to determine the KC-EryK structure. In the case of CLT-EryK, molecular replacement was carried out to determine the initial crystallographic phases using the program MolRep (*24*), from the CCP4 suite (*25*), by using the open ligand-free structure of EryK as search model (PDB accession code 2WIO (*16*, *21*)). In both cases refinement was carried out with Refmac5 in CCP4 (*26*), followed by model building and manual adjustment performed by COOT (*27*, *28*). Solvent molecules were added into the $F_o - F_c$ density maps, contoured at 3σ, with the FIND WATERS tool of COOT. Five percent of the reflections were excluded from refinement for cross-validation by means of free *R*-factor (*29*). Secondary structure assignment was performed using the Kabsch and Sander algorithm, and the geometrical quality of final models was assessed using PROCHECK (*30*). Ramachandran statistics indicate no outliers for the KC-EryK structure: only one amino acid, Ile392, is close to the forbidden region for the CLT-EryK structure. This residue was previously found to be in a similar conformation in the closed structures of EryK, both ligand free and in complex with ErD (*16*). The first 15 N-terminal residues in KC-EryK and 17 N-terminal residues in CLT-EryK are missing in the models due to insufficient electron density. Final crystallographic statistics are shown in Table 1. All figures were produced with PyMOL (http://pymol.sourceforge.net). The atomic coordinates and structure factors for the two crystal forms presented here (KC-EryK at 2.0 Å and CLT-EryK at 1.9 Å) have been deposited in the RCSB Protein Data Bank (accession codes 2JJP and 2XFH).

Equilibrium Binding Analysis. Binding affinities of both KC and CLT to EryK were determined at 298 K by titrating the enzyme at a concentration of 2.0 and 0.4 μM, respectively, using a final volume of 800 μL of 50 mM Tris·HCl, pH 7.5. The P450 inhibitors KC and CLT were prepared as stock solutions (respectively 20 and 10 mM) in DMSO. The final ligand concentration covered a range from 0 to 30 μM for KC and from 0 to 8 μM for CLT; in these ranges the final percentage of DMSO was maintained under 1%. The absorption shift induced by ligand binding was probed by collecting UV−visible spectra, recorded between 250 and 820 nm, after each substrate addition. The inhibitor binding process was monitored by following the absorption shift of the heme Soret peak of EryK from 417 to 435 nm, caused by the coordination of azole nitrogen to the heme iron (Figure 2). From each of the ligand-bound spectrum the appropriate blank spectrum was subtracted.

Absorbance intensities at 420 nm were plotted against the added inhibitor concentration (Figure 2). The dissociation constants (K_d) were estimated using Kaleidagraph software package.

Since the K_d values of the azole drugs were not markedly higher than the concentration of EryK used, data were fitted to the quadratic equation:

$$\Delta AU_{obs} = \frac{\Delta AU_{max}}{2}([E_0]+[I_0]+K_d - (([E_0]+[I_0]+K_d)^2 - 4([E_0][I_0]))^{1/2}) \quad (1)$$

where ΔAU_{obs} is the absorbance difference, ΔAU_{max} is the maximum absorbance difference extrapolated to infinite inhibitor concentration, and $[E_0]$ and $[I_0]$ are the enzyme and the inhibitor analytical concentrations, respectively. Data were also globally fitted with the program Prism (Graphpad).

Table 1: Data Collections, Refinement Statistics, and Validation[a]

protein	KC-EryK	CLT-EryK
crystallization condition	2.0 M $(NH_4)_2SO_4$, 0.1 M Bis-Tris, pH 6.5	25% PEG 3350, 0.1 M Hepes, pH 7.0, 0.2 M NaCl
data collection		
resolution (Å)	50.0−2.00 (2.15−2.00)	50.0−1.9 (1.97−1.90)
total measurements	126637	311184
unique reflections	25326	36185
completeness (%)	91.4 (85.70)	94.0 (84.4)
redundancy	3.9 (3.30)	2.9 (2.80)
R_{merge}[b] (%)	4.8 (19.40)	12.1 (37.4)
$I/\sigma(I)$	16.5 (12.70)	8.8 (2.16)
Wilson B-value (Å^2)	22.7	20.2
refinement		
resolution (Å)	56.7−2.10 (2.15−2.00)	42.8−1.9 (1.97−1.90)
reflections	20602	33096
molecules per asymmetric unit	1	1
space group	$P2_1$	$P1$
unit cell (Å; deg)	$a = 53.24$, $b = 68.04$, $c = 57.69$; $\beta = 100.71$	$a = 37.92$, $b = 53.68$, $c = 58.11$; $\alpha = 100.27$, $\beta = 90.93$, $\gamma = 94.19$
R_{cryst}/R_{free}[c] (%)	19.9/26.2	18.1/23.0
mean B-factors (Å^2)		
protein	32.1	25.8
heme	18.3	16.8
substrate	49.0	24.1
water/iron	33.9/19.35	34.2/18.7
deviation from ideal geometry		
bond (Å)	0.016	0.014
angles (deg)	1.611	1.582
Ramachandran (%) , most favored/ allowed/outliers	85.5/13.5	96.4/3.6/0.2
no. of atoms		
protein	3152	3868
heme/ligand	43/36	43/25*2
water/sulfate/DMSO	232/10/0	389/0/10
solvent content (%)	41.3	42.1

[a]Highest-resolution shell is shown in parentheses. [b]$R_{merge} = \sum_i \sum_j |I_{i,j} - \langle I_j \rangle| / \sum_i \sum_j I_{i,j}$, where i runs over multiple observations of the same intensity and j runs over all crystallographically unique intensities. [c]$R_{cryst} = \sum ||F_o| - |F_c|| / \sum |F_o|$, where $|F_o| > 0$. R_{free} is based on 5% of the data randomly selected and is not used in the refinement.

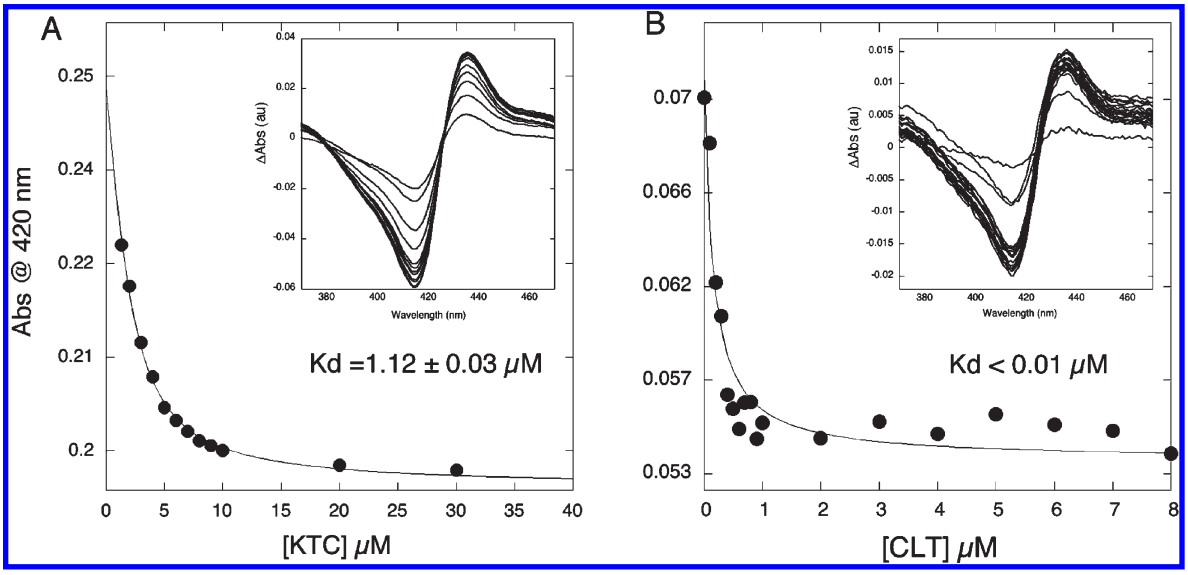

FIGURE 2: Equilibrium binding titrations of EryK with ketoconazole (KC) and clotrimazole (CLT). Both KC (panel A) and CLT (panel B) induce on EryK the typical type II spectral shift of the Soret peak that occurs during the binding of azole inhibitors to P450s. Absorbance and difference spectra as a function of concentration of inhibitors are given for KC (panel A and relative inset) and for CLT (panel B and relative inset). In each experiment absorbance was monitored at 420 nm using a constant EryK concentration (2.0 and 0.4 μM for binding titration with KC and CLT, respectively) at 298 K in 50 mM Tris·HCl, pH 7.5. Since the value of K_d for CLT is in the nanomolar range, in order to determine this parameter reliably, we had to decrease the concentration of EryK, at the expense of the signal-to-noise ratio. Data were fitted to eq 1 (fits are shown as solid lines) to determine the dissociation constants, K_d.

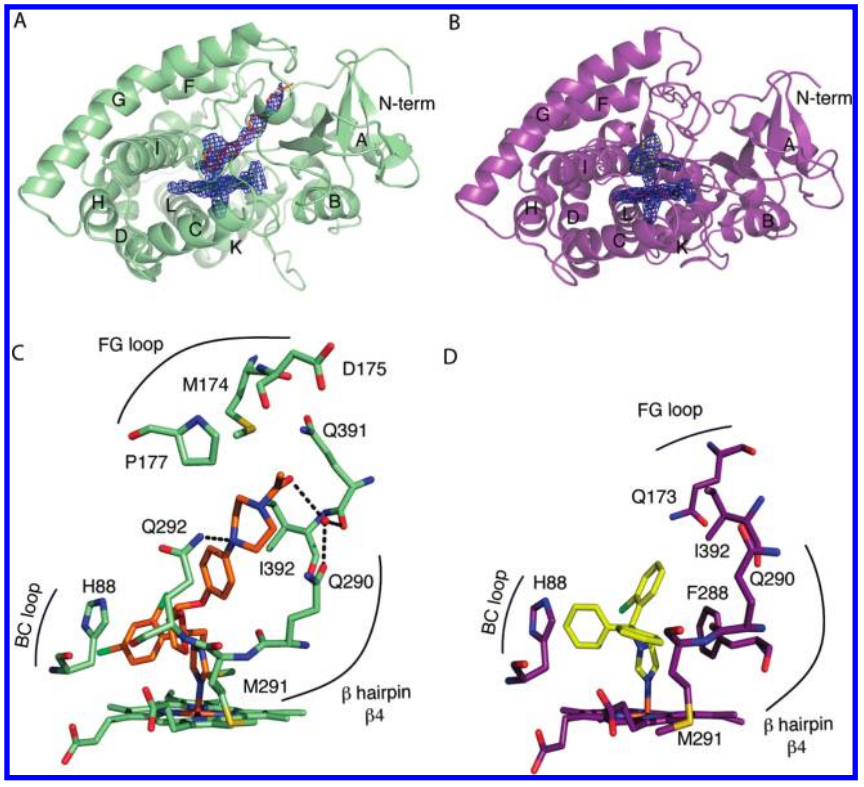

FIGURE 3: Ketoconazole (KC) and clotrimazole (CLT) in the active site of EryK. The overall structures of EryK in complex with KC (KC-EryK, green ribbon, panel A) and CLT (CLT-EryK, purple ribbon, panel B) and the electron density omit maps are given. The maps are contoured at 1σ around the heme group, Cys353, KC (orange, panel A), and CLT (yellow, panel B). Azole coordination to the iron is visible as a continuous electron density in both maps. In both panels EryK is not shown in the standard P450 orientation but in the orientation that allows clear visualization of the inhibitors bound into the active site. Amino acids interacting with KC (orange, panel C) and CLT (yellow, panel D) are shown. The heme group and the residues located within 4.5 Å of KC and 5.0 Å of CLT are shown as sticks (carbon atoms colored green and purple, respectively, for the complex KC-EryK and for the complex CLT-EryK). A water molecule (H_2O 20) is represented as a red sphere. Black dashed lines indicate hydrogen bonds in all panels. Capital letters indicate the secondary structure elements according to P450 nomenclature.

RESULTS AND DISCUSSION

Equilibrium Binding Analysis. Equilibrium binding titrations of EryK with KC and CLT, followed by optical spectroscopy, yield for KC a K_d value of 1.12 ± 0.03 μM, whereas for CLT we estimate a K_d smaller than 0.01 μM (Figure 2). Since the value of K_d for CLT is in the nanomolar range, in order to determine this parameter reliably, we had to decrease the concentration of EryK at the expense of the signal-to-noise ratio.

Both inhibitors bind EryK with an affinity higher than ErD (K_d = 3.5 ± 0.1 μM (*16*)), especially CLT. Even though both inhibitors present an imidazole group binding to the heme iron of the enzyme, their N1 substituents on the ring are structurally and chemically different (Figure 1). A detailed description of the structural features of the interaction of EryK with the two ligands is given below.

KC-EryK and CLT-EryK Crystal Structures. Crystals of EryK in complex with KC and CLT, diffracting respectively to 2.1 and 1.9 Å resolution, were grown by cocrystallization using a saturating concentration of the inhibitors (see Experimental Procedures and ref *21*). Refinement of the KC-EryK model gave R_{cryst} = 19.9% and R_{free} = 26.2%. The refinement of the protein in complex with CLT gave R_{cryst} = 18.1% and R_{free} = 23.0%.

The initial electron density omit maps, calculated without inclusion of inhibitors in the model, revealed clear electron density in the active site corresponding to KC in one case and CLT in the other (Figure 3A,B). In the CLT-EryK structure additional weak electron density was found on the top of the first CLT molecule coordinated to the heme iron. We interpreted this density as a second molecule of CLT that enters aspecifically into the active site of EryK, since it is present in the crystallization solution as large excess. Indeed, this electron density can be accounted for by a CLT molecule in two orientations with a total occupancy of 50%, without establishing significant contacts with residues present in the active site. Moreover, the curve obtained by equilibrium binding experiments fits best to a hyperbolic equation, which indicates a single binding event (Figure 2B). For these reasons, we conclude that the presence of a second molecule of CLT into the active site is not relevant for EryK inhibition and that the open conformation in which CLT stabilizes EryK allows another molecule of CLT to be trapped in the crystal.

In both closed and open structures of ligand-free EryK the sixth coordination position of the heme iron is occupied by a water molecule with a bond length of 2.3 Å (*16*). In KC-EryK and CLT-EryK the two azoles displace this water molecule and are directly bound to the heme. Azole coordination to the iron was visible as a continuous electron density in both maps (Figure 3A, B). The coordination bond distances between the N3 of the imidazole ring and ferric iron atom are 1.96 Å in KC-EryK and 2.10 Å in CLT-EryK structure.

Binding with KC induces the closure of the enzyme; indeed, rmsd after superposition of KC-EryK and ligand-free closed EryK yields a value of 1.4 Å for C_α carbons. In the KC-EryK structure the long N1 substituent is located within the access channel of the enzyme; it adopts a roughly straight conformation, lying on the fixed region of EryK binding site and establishing hydrophobic interactions with some residues of the FG loop, a mobile segment (Figure 3C).

The fixed region in the active site of EryK, formed by the loop at the C-terminal of helix K and the β-hairpins β4 and β1, was previously found to be responsible for the recognition of the desosamine sugar of ErD. The desosamine moiety establishes two H-bonds with Gln292 and, through a water molecule, with Gln290 (*16*). KC can mimic these interactions since (i) the tertiary amine N4 of the piperazine ring of KC forms a direct H-bond with the side chain of Gln292 on the β-hairpin β4 and (ii) the terminal keto group of its N1 acetyl moiety forms a H-bond with a bridging water (H_2O 20) bound to the $O\varepsilon_1$ of Gln290 on the C-terminal loop of helix K and to the carbonyl group of the main chain of Gln391 on the C-terminal region (Figure 3C).

Furthermore, the presence of KC induces a movement of the FG loop on the top of the active site of about 9 Å, similar to what was observed in the closed EryK structures. Only three residues on this loop, Met174, Asp175, and Pro177, assume a different conformation with respect to closed EryK, both ligand free and in complex with ErD, being in contact with the acetyl moiety of KC (Figure 3C).

The overall structure of CLT-EryK closely resembles the open ligand-free structure with a rmsd after superposition of 0.98 Å. In CLT-EryK, the short but bulky structure of CLT lies over the heme group, establishing hydrophobic contacts with residues located on the FG loop (Gln173), the β-hairpins β4 (Phe288, Gln290, Met291), and the C-terminal region (Ile392) (Figure 3D).

In both inhibitor-bound structures, the imidazole ring of His88 on the BC loop establishes a stacking interaction respectively with the dichlorophenyl ring of KC and with one of the phenyl ring of CLT (Figure 3C,D). This amino acid in the structure of EryK bound to ErD (ErD-EryK, PDB code 2JJO (*16*)) interacts with the mycarose moiety of ErD by H-bonding. By comparing these three bound structures, we observed that the side chain of His88, regardless of the structure of the molecule bound in the active site, conserves its position and is in contact with the ligand.

KC and CLT Select for Alternative Conformations of EryK. The structures of EryK in complex with KC and CLT showed that the N1-substituent groups on the imidazole moiety can induce on EryK different responses, stabilizing the P450−inhibitor complex in an open or in a closed conformation.

Structural analysis of two ligand-free structures of EryK has shown the existence of open and closed forms of the enzyme that are in equilibrium in solution. Functional studies carried out by stopped-flow rapid mixing experiments also supported the presence of open and closed protein conformations, whose relative populations can be shifted by a ionic strength range that parallels crystallization conditions of the two states (*16*). The main features of the closed ligand-free EryK structure are that (i) the BC and the FG loops move in concert by 10 Å each to close the access channel, (ii) helix G is kinked at the level of Pro192, and (iii) helix F is unwound from the N-terminal end to Asp163. The structure of ErD-EryK resembles the closed ligand-free EryK conformation but with some specific differences due to the presence of the bulky substrate in the active site. In ErD-EryK, the BC loop movement is less pronounced and, even if the movement of FG loop is similar and helix G is kinked, helix F is not unwound (*16*). These concerted movements are a consequence of helix I bending, due to the extensive interactions that the macrolactone ring of ErD establishes with side chains in its middle groove (Ala237, Leu240, Ala241, Ile244, Thr245). As also reported for other P450s (*31*), helix I bending is characterized by the loss of two main chain helical hydrogen bonds, which leads to a helical pitch of ~7 Å. This induces the formation of a cleft that has been proposed to provide space for binding of dioxygen and water during the catalytic reaction (Supporting Information Figure S2). Furthermore, in ErD-EryK, bending of helix I induces flipping and reorientation of His243 on helix I itself that can establish a H-bond with Ser166, located on helix F. This interaction is coupled to a shift of helix F and causes Trp165 to exert a pressure at the level of Pro192 on helix G, which kinks. Helix G kinking drives the FG loop in hydrophobic contact with the BC loop, resulting in closure of the access to the active site. This network of interactions (HSWP network) locks the helix G kinking. In the open conformation of ligand-free EryK, the HSWP network is also present, although with a different geometry that does not induce helix G kinking and prevents helix F to unwind. On the other hand, in the ligand-free EryK closed structure, the HSWP network is absent; therefore, these interactions favor the open conformation in the absence of the substrate and stabilize the closed one in its presence (*16*).

In the structures of EryK in complex with KC and CLT the presence on the heme group of the two azole inhibitors was found to affect its opening and closing mechanism, depending on the ligand, as we will detail in the next paragraph.

Upon KC binding, EryK rearranges similarly to what was observed in the structure of its ligand-free closed form: helix F shows a pronounced unwinding from the N-terminus to Phe162 and helix G is kinked (Figure 4A). On the other hand, the CLT-EryK structure closely corresponds to the structure of its ligand-free open form: helix F is fully structured and helix G is not kinked (Figure 4B).

The structural response that occurs upon binding of inhibitors is triggered by the distortion of helix I that lines the active site and is affected by ligands. Flexibility of helix I represents a common feature in the P450 family. The capability to arrange in multiple conformations allows this helix to be ligand-responsive (*32*, *33*). In the case of EryK, substrate and inhibitors establish hydrophobic contacts with the central residues of helix I, but in the complexes with KC and CLT, the imidazole group, constrained by the coordination bond at a fixed distance and geometry, introduces a bulk that is absent in the ErD-EryK complex. This hindrance is concentrated at the level of Ala241 that undergoes a displacement of about 2 Å, more pronounced than in the case of ErD-EryK. Nevertheless, this local point hindrance is dissipated by the distortion of only one helical turn, whereas the extensive, although locally less constrained, contacts with ErD induce an overall bending of helix I. As a result, in KC-EryK and CLT-EryK, the C- and the N-terminal sections of the helix are substantially unchanged, in spite of the rearrangement around Ala241. A similar distortion of helix I at the level of an alanine in this topological position was found in the structures of P450EryF, P4503A4, and P450BM3 in complex with imidazole inhibitors (*12*, *32*, *34*). In EryK, as reported also for P450BM3, the presence of a glycine following this alanine confers conformational flexibility to the helix I backbone in this region. Such a flexibility allows Ala241 to move away from the inhibitors, inducing significant ligand-dependent changes in the positions of Gly242, His243, Ile244, and Thr245.

In the case of KC, the hydrophobic interactions that it establishes with helix I are mostly concentrated at the level of residues before Ala241 (Ala237, Leu240, Ala241, Thr245), and the helix I distortion implies a reorientation of His243 (Figure 4C). Furthermore, the terminal acetyl moiety of KC interacts with Met174 and Asp175 on the top of the FG loop. The strain introduced by the movement of the FG loop, in contact with the terminal part of

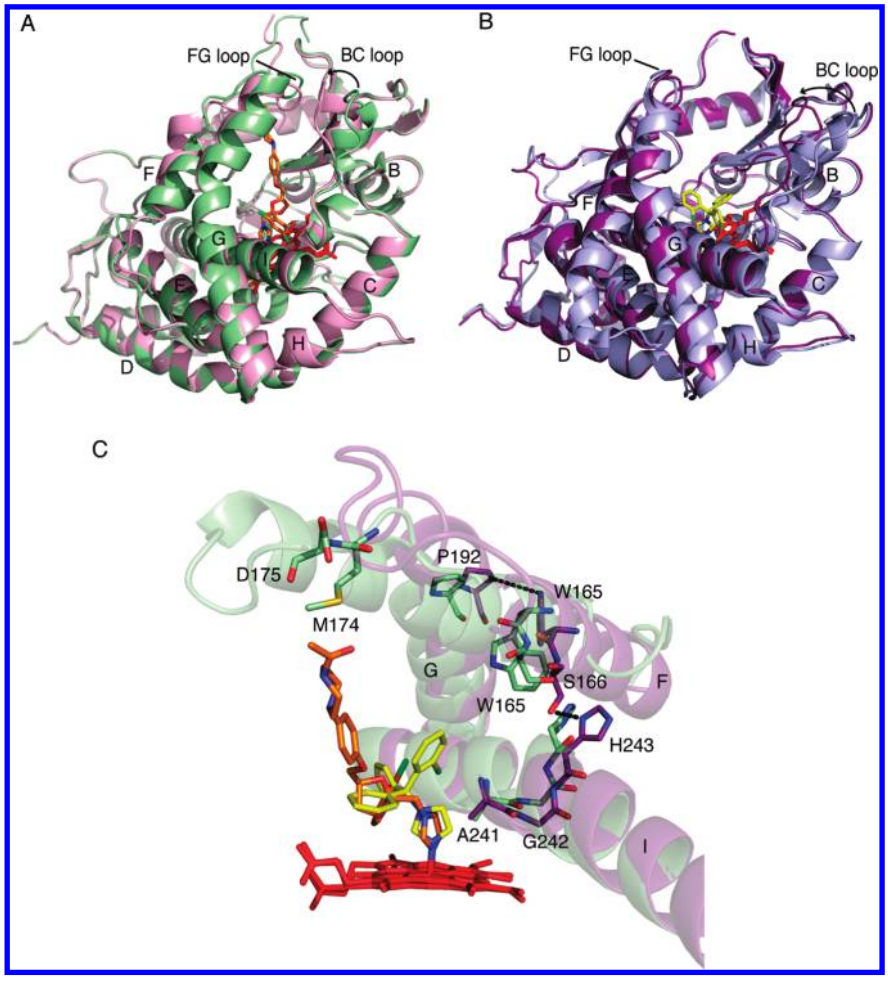

FIGURE 4: Panels A and B: Secondary structure superposition of KC-EryK and CLT-EryK with the EryK ligand-free structures. KC-EryK (green ribbon) superposed to the closed ligand-free structure of EryK (pink ribbon, PDB code 2JJN) is shown in panel A. Ketoconazole and heme are represented as sticks in orange and red, respectively. CLT-EryK (purple ribbon) superposed to the open ligand-free structure of EryK (light blue ribbon, PDB code 2WIO) is shown in panel B. Clotrimazole and heme are represented as sticks in yellow and red, respectively. Panel C: Overview of the HSWP network. The superposition of the HSWP network of KC-EryK (green) and CLT-EryK (purple) is shown. The long chain of the N1-substituent group of KC (orange sticks) spans from the central region of helix I to the C-terminal part of helix F, establishing interactions that prevent the HSWP network to be formed. On the other hand, CLT (yellow sticks) fits the distal pocket of EryK inducing a local distortion of helix I but retaining the HSWP network in a geometry that locks EryK in an open conformation. Heme groups are given in red. Carbon atoms of amino acids are given in green for KC-EryK and purple for CLT-EryK. Dashed lines indicate the HSWP interaction.

KC, pulls up helix F from its C-terminal region and determines a displacement of Ser166, causing the loss of the H-bond with His243 on helix I. As a consequence, Trp165 rotates and docks in a position pointing toward helix I with an interaction with His243 (Figure 4C). Therefore, helix F unwinds, assuming a random-coil structure, due to the disruption of the HSWP network. A similar organization of the HSWP network has been observed in the ligand-free closed structure (Supporting Information Figure S1A,B), that is accordingly unfavored in solution with respect to the ligand-free open conformer, where the HSWP network is present. Moreover, in KC-EryK, the rearrangement of helix I determines the loss of the helix I cleft, that is shifted and exposed on the opposite side with respect to the heme group (Supporting Information Figure S2).

In CLT-EryK, the inhibitor interacts more extensively than KC with residues following Ala241 (Ala237, Ala241, Ile244, Thr245) due to the orientation of the imidazole ring (Figure 4C) and to the chlorophenyl ring that points toward helix I. In spite of the distortion of helix I, we observed that, in CLT-EryK, His243 maintains the H-bond with Ser166 and the HSWP network is present with the same geometry found in the ligand-free open form of EryK, including a structured helix F and helix G without a kink (Figure 4B,C; for more details see Supporting Information Figure S1). Furthermore, in CLT-EryK, the distortion of helix I does not disrupt helical hydrogen bonds, resulting in the absence of the catalytic cleft (Supporting Information Figure S2). A local repositioning of the helical backbone was previously noted also in the helix I structure of P450EryF in complex with KC (*32*).

In conclusion, the azole inhibitors interact with helix I and activate a cascade of events at the level of helices F and G that shift the equilibrium between the open and the closed form of EryK, selectively trapping the enzyme in the different conformers, according to the bound inhibitor.

These considerations may provide an explanation for the apparent inconsistency that the ligand that stabilizes a "closed" conformation is characterized by a 2 orders of magnitude higher K_d value. The conformation selected by CLT, in spite of being open-like, is characterized, among others, by additional stability due to the presence of the HSWP network, as already observed in solution by equilibrium measurements (*16*).

Moreover, inspection of KC-EryK and CLT-EryK revealed a significant variation of the BC loop conformation with respect to

both the open and closed ligand-free EryK structures. Indeed, by analyzing the rmsd between closed ligand-free EryK vs closed KC-EryK and between open ligand-free EryK vs open CLT-EryK, we observed a displacement of more than 6 Å at the level of the BC loop, between Pro73 and Pro82. This protein region appears to be mobile and, in the absence of direct contacts with bound ligands or with the lattice, that could select a fully open or closed conformation, an intermediate position is observed for this loop. This is confirmed by the presence of two conformers in CLT-EryK and by the not well-defined electron density in the region from Arg75 to Pro82, in both KC-EryK and CLT-EryK.

CONCLUDING REMARKS

The structures of EryK in complex with two chemically different azole inhibitors provide an example of P450 inhibition that is rationalized by a conformational selection model, showing a case in which a high inhibition is coupled to an open conformation of the active site. Depending on the inhibitor, EryK adopts two conformations that correspond to the ones observed in the absence of ligands (*16*): when bound to KC, the protein switches to a state analogous to the closed ligand-free one; on the contrary, binding with CLT locks EryK in an open conformation.

The conformational selection model, previously proposed for the ligand binding mechanism of EryK, is confirmed by these results. The structures of EryK bound to KC and CLT reveal the ability of ligands to shift the equilibrium between the open and the closed ligand-free conformers (*16*). According to this model, binding can occur only to the fraction of EryK molecules that are in the open ligand-free state. Upon binding, helix I triggers a response of the whole structure by changing the geometry of the HSWP network. The transition experienced by EryK depends on the state of this network: if it is disrupted, the molecule closes but does not lock; if the network is in the configuration corresponding to the open state, the structure stays in the open form, in spite of the presence of a ligand in the active site.

Recently, other P450s were found to explore alternative ligand-free conformations (*17*, *18*, *20*). Here we show that it is possible to stabilize two conformational states by exploiting widely used drugs, such as azole inhibitors.

In addition, this study stresses the importance of determining the crystal structures of P450s in complex with ligands, especially inhibitors, with the aim to improve drug design being aware of the protein−ligand interactions and the conformational changes explored by the protein structure.

ACKNOWLEDGMENT

We acknowledge the Helmholtz-Zentrum Berlin electron storage ring BESSY II and the European Synchrotron Radiation Facility for provision of synchrotron radiation at beamlines ID14.1 and ID14.3, respectively. We thank M. Fornara for skillful support during experimental manipulations.

SUPPORTING INFORMATION AVAILABLE

Figure S1, a detailed representation of the HSWP network; Figure S2, the structural details of the ligand-dependent changes on the helix I cleft. This material is available free of charge via the Internet at http://pubs.acs.org.

REFERENCES

1. Denisov, I. G., Makris, T. M., Sligar, S. G., and Schilichting, I. (2005) Structure and chemistry of cytochrome P450. *Chem. Rev. 105*, 2253–2277.
2. Meunier, B., de Visser, S. P., and Shaik, S. (2004) Mechanism of oxidation reactions catalyzed by cytochrome p450 enzymes. *Chem. Rev. 104*, 3947–3980.
3. Pylypenko, O., and Schlichting, I. (2004) Structural aspects of ligand binding to and electron transfer in bacterial and fungal P450s. *Annu. Rev. Biochem. 73*, 991–1018.
4. Wreck-Reichhart, D., and Feyereisen, R. (2000) Cytochromes P450: a success story. *Genome Biol. 1*, 1–9.
5. Lamb, D. C., Waterman, M. R., Kelly, S. L., and Guengerich, F. P. (2007) Cytochromes P450 and drug discovery. *Curr. Opin. Biotechnol. 18*, 504–512.
6. McLean, K. J., Marshall, K. R., Richmond, A., Hunter, I. S., Fowler, K., Kieser, T., Gurcha, S. S., Besra, G. S., and Munro, A. W. (2002) Azole antifungals are potent inhibitors of cytochrome P450 monooxygenases and bacterial growth in mycobacteria and streptomyces. *Microbiology 148*, 2937–2949.
7. Schuster, I., and Bernhardt, R. (2007) Inhibition of cytochrome P450: existing and new promising therapeutic targets. *Drug Metab. Rev. 39*, 481–499.
8. Thiel, K. A. (2004) Structure-aided drug design's next generation. *Nat. Biotechnol. 22*, 513–519.
9. Kalb, V. F., Woods, C. W., Turi, T. G., Dey, C. R., Sutter, T. R., and Loper, J. C. (1987) Primary structure of P450 lanosterol demethylase gene from Saccharomyces cerevisiae. *DNA 6*, 529–537.
10. Balding, P. R., Porro, C. S., McLean, K. J., Sutcliffe, M. J., Maréchal, J.-D., Munro, A. W., and de Visser, S. P. (2008) How do azoles inhibit cytochrome P450 enzymes? A density functional study. *J. Phys. Chem. A 112*, 12911–12918.
11. Aoyama, Y., Kudo, M., Asai, K., Okonogi, K., Horiuchi, T., Gotoh, O., and Yoshida, Y. (2000) Emergence of fluconazole-resistant sterol 14-demethylase P450 (CYP51) in *Candida albicans* is a model demonstrating the diversification mechanism of P450. *Arch. Biochem. Biophys. 379*, 170–171.
12. Haines, D. C., Chen, B., Tomchick, D. R., Bondlela, M., Hegde, A., Machius, M., and Peterson, J. A. (2008) Crystal structure of inhibitor-bound P450BM-3 reveals open conformation of substrate access channel. *Biochemistry 47*, 3662–3670.
13. Locuson, C. W., Hutzler, J. M., and Tracy, T. S. (2007) Visible spectra of type II cytochrome P450-drug complexes: evidence that "incomplete" heme coordination in common. *Drug Metab. Dispos. 35*, 614–622.
14. Zhang, W., Ramamoorthy, Y., Kilicarslan, T., Nolte, H., Tyndale, R. F., and Sellers, E. M. (2002) Inhibition of cytochrome P450 by antifungal imidazole derivatives. *Drug Metab. Dispos. 30*, 314–318.
15. Lambalot, R. H., Cane, D. E., Aparicio, J. J., and Katz, L. (1995) Overproduction and characterization of the erythromycin C-12 hydroxylase, EryK. *Biochemistry 34*, 1858–1866.
16. Savino, C., Montemiglio, L. C., Sciara, G., Miele, A. E., Kendrew, S. G., Jemth, P., Gianni, S., and Vallone, B. (2009) Investigating the structural plasticity of a cytochrome P450: three-dimensional structures of P450 EryK and binding to its physiological substrate. *J. Biol. Chem. 284*, 29170–29179.
17. Lampe, J. N., Brandman, R., Sivaramakrishnan, S., and Ortiz de Montellano, P. R. (2010) Two-dimensional NMR and all-atom molecular dynamics of cytochrome P450 CYP119 reveal hidden conformational substates. *J. Biol. Chem. 285*, 9594–9603.
18. Lee, Y.-T., Wilson, R. F., Rupniewski, I., and Goodin, D. B. (2010) P450cam visits an open conformation in the absence of substrate. *Biochemistry 49*, 3412–3419.
19. Muralidhara, B. K., Negi, S., Chin, C. C., and Braun, Halpert J.R. (2006) Conformational flexibility of mammalian cytochrome P450 2B4 in binding imidazole inhibitors with different ring chemistry and side chains. *J. Biol. Chem. 281*, 8051–8061.
20. Sherman, D. H., Li, S., Yermalitskaya, L. V., Kim, Y., Smith, J. A., Waterman, M. R., and Podust, L. M. (2006) The structural basis for substrate anchoring, active site selectivity, and product formation by P450 PikC from *Streptomyces venezuelae*. *J. Biol. Chem. 281*, 26289–26297.
21. Savino, C., Sciara, G., Miele, A. E., Kendrew, S. G., and Vallone, B. (2008) Cloning, expression, purification, crystallization and preliminary X-ray crystallographic analysis of C-12 hydroxylase EryK from *Saccharopolyspora erythraea*. *Protein Pept. Lett. 15*, 1138–1141.
22. Otwinowski, Z., and Minor, W. (1997) Processing of X-ray diffraction data collected in oscillation mode. *Methods Enzymol. 276*, 307–326.

23. Minor, W., Tomchick, D., and Otwinoski, Z. (2000) Strategies for macromolecular synchrotron crystallography. *Structure 8*, R105–110.
24. Vagin, A., and Teplyakov, A. (1998) A translation-function approach for heavy-atom location in macromolecular crystallography. *Acta Crystallogr., Sect. D: Biol. Crystallogr. 54*, 400–402.
25. Collaborative Computational Project, N. (1994) The CCP4 suite: programs for protein crystallography. *Acta Crystallogr., Sect. D: Biol. Crystallogr. 50*, 7690–7763.
26. Pannu, N. J., Murshudov, G. N., Dodson, E. J., and Read, R. J. (1998) Incorporation of prior phase information strengthens maximum-likelihood structure refinement. *Acta Crystallogr., Sect. D: Biol. Crystallogr. 54*, 1285–1294.
27. Emsley, P., Lohkamp, B., Scott, W. G., and Cowtan, K. (2010) Features and Development of Coot. *Acta Crystallogr., Sect. D: Biol. Crystallogr. 66*, 486–501.
28. Emsley, P., and Cowtan, K. (2004) Coot: model-building tools for molecular graphics. *Acta Crystallogr. D60*, 2126–2132.
29. Brunger, A. T. (1992) Free R value: a novel statistical quantity for assessing the accuracy of crystal structures. *Nature 355*, 472–475.
30. Laskowski, R. A., Moss, D. S., and Thornton, J. M. (1993) Main-chain bond lengths and bond angles in protein structures. *J. Mol. Biol. 231*, 1049–1067.
31. Cupp-Vickery, J. R., and Poulos, T. L. (1995) Structure of cytochrome P450eryF involved in erythromycin biosynthesis. *Nat. Struct. Biol. 2*, 144–153.
32. Cupp-Vickery, J. R., Garcia, C., Hofacre, A., and McGee-Estrada, K. (2001) Ketoconazole-induced conformational changes in the active site of cytochrome P450eryF. *J. Mol. Biol. 311*, 101–110.
33. Strushkevich, N., Usanov, S. A., and Park, H.-W. (2010) Structural basis of human CYP51 inhibition by antifungal azoles. *J. Mol. Biol. 397*, 1067–1078.
34. Ekroos, M., and Sjogren, T. (2006) Structural basis for ligand promiscuity in cytochrome P450 3A4. *Proc. Natl. Acad. Sci. U.S.A. 103*, 13682–13687.